

SAPPLEMENTARY MATERIALS AND METHODS

Mouse antibodies for flow cytometry and *in vivo* assays. Anti-CD8 (clone 53-6.7), anti-CD4 (clone:RM4-5), anti-CD3 (clone:17A2), anti-CD45 (clone 30-F11), anti-CD25 (clone PC61), anti-CD357 (clone YG1TR 765), anti-CD223 (clone C9B7W), anti-CD69 (clone H1.2F3), anti-CD279 (clone 29F.1A.12), anti-CD137 (clone 17B5), anti-CD366 (B8.2C12), anti-CD49b (clone:DX5), anti-FOXP3 (MF-14), anti-F4/80 (clone:BM8), anti-CD11b (clone:M1/70), anti-CD11c (clone:N418), anti-CD206 (clone:C068C2), anti-CD80 (clone:16-10A1), anti-Ly-6C (clone:HK1.4) anti-I-A/I-E (clone:M5/114.15.2), anti-Ly-6G/Ly-6C (clone: RB6-8C5) and anti-IFN- γ (clone XMG1.2) were purchased from BioLegend. *In vivo* MAb anti-CD8 (clone:53-6.7) were purchased from BioXcell. The anti-mouse PD-1 (clone RMP1-14) was produced in-house from hybridomas and was purified using a protein G column.

Antibodies used for phospho-flow cytometry. Phospho-mTOR (Ser2448) antibody (clone MRRBY) was purchased from eBioscience. Phospho-Akt (Ser473) antibody (clone D9E) was purchased from Cell Signaling Technology.

Human flow cytometry antibodies. Anti-CD8 (clone SK1), anti-CD25 (clone BC96), anti-CD223 (clone 11C3C65), anti-CD69 (clone FN50), anti-CD279 (clone A17188B), and anti-IFN- γ – (clone

B27) were purchased from BioLegend.

Flow cytometric analysis and intracellular cytokine staining. Cell suspensions prepared from tumors and spleens were stained for surface markers using antibodies at the appropriate concentrations in PBS containing 2% FBS for 15 min at 4 °C. To assess cell proliferation, cells were stained with 1 μM of CellTrace Far Red Cell Proliferation Dye (Thermo Fisher Scientific) or carboxyfluorescein succinimidyl ester (CFSE). For intracellular cytokine staining, cells were incubated for 6 h with GolgiPlug (BD Biosciences) and were stained with surface markers. After permeabilization and fixation using a Cytofix/Cytoperm Kit (BD Biosciences), the cells were stained with antibodies. For phospho-specific flow cytometry, cells were fixed for 20 min at room temperature with Phosflow Fix Buffer I (BD Biosciences), stained for surface markers, and then permeabilized for 15 min at 4°C with Phosflow Perm Buffer III (BD Biosciences). After washing, these cells were incubated with the phospho-antibodies. All samples were analyzed on a FACS Canto II system (BD Biosciences) using FlowJo software (BD Biosciences).

Docking studies. Docking studies were conducted using the MOE 2019.0102 software. The three-dimensional structure of NADH dehydrogenase FMN-binding site of mouse mitochondrial complex I was obtained from the protein data bank (PDB Id: 6ZR2). During docking analysis using MOE, the structure was hydrogenated using the Protonate 3D module. After partial charges were assigned using

an all-atom force field combining Amber10 and Extended Hueckel Theory (EHT), hydrogen atoms were minimized. The Alpha Site Finder module was used for definition of a FMN binding site. PQDN and FMN generated using the stochastic search method were docked on the binding site. Docked poses were optimized using the Amber10: EHT force field, and ranked according to the GBVI/WSA scoring function which estimates the free energy of binding of the ligand from a given pose.

RNA sequencing. Total RNA was extracted from whole splenocytes from DUC18 cultured for 24 h. Prepared RNA was quantified using spectrophotometry, while the RNA quality was confirmed using Bioanalyzer 2100 (Agilent Technologies). The mRNA was prepared from total RNA and the NGS library using Colibri 3'mRNA Library Prep kit for illumina Systems according to manufacture's instructions (Thermo Fisher Scientific). RNA-Seq was performed using Miseq (Illumina), resulting in 10 million (2×75 bp) reads from each library. Sequencing reads were analyzed using the MASER pipeline platform. Filtered reads were aligned to the mouse mm10 genome using TopHat2; the expression levels per sample were analyzed using Cufflinks. RNA-Seq data are available on the DDBJ (E-GEAD-456).

Detection of mitochondrial membrane potential using TMRE. Cells were seeded into 96-well

plates at 1×10^5 cells/well. At each time point, cells were incubated with 100 nM of TMRE (Abcam) for 45 min at 37 °C. The mean fluorescence intensity of TMRE was determined using flow cytometry.

TCR repertoire analysis. TCR-seq libraries for next-generation sequencing (NGS) were prepared from the mRNA of sorted T cell samples. Total mRNA was converted to cDNA using reverse transcriptase, and universal sequences for unbiased PCR amplification were added to the 5' end by poly-A tailing with the terminal deoxynucleotidyl transferase reaction and subsequent second strand synthesis using a universal primer. The TCR locus was amplified by nested PCR using universal primers and TCR constant region-specific primers. Amplified TCR libraries were then enzymatically fragmented, and sequencing adaptors and barcodes were added to the TCR libraries using ligation and subsequent PCR. Final TCR libraries with 200–300 base pairs were sequenced using an Ion Proton next-generation sequencer (Thermo Fisher Scientific).

Alignment and assembly of TCR-seq data. Sequencing data were processed using MiXCR-1.8.2.¹ Adapter sequences and low-quality reads were trimmed using cutadapt-v1.11 and PRINSEQ-0.20.4. Filtered reads were aligned to the ImMunoGeneTics (IMGT) reference mouse TCR V/D/J sequences with the following parameters: `-OvParameters.geneFeatureToAlign = VTranscript -OvjAlignmentOrder = JThenV`. Identical sequences were then assembled and grouped into clones by

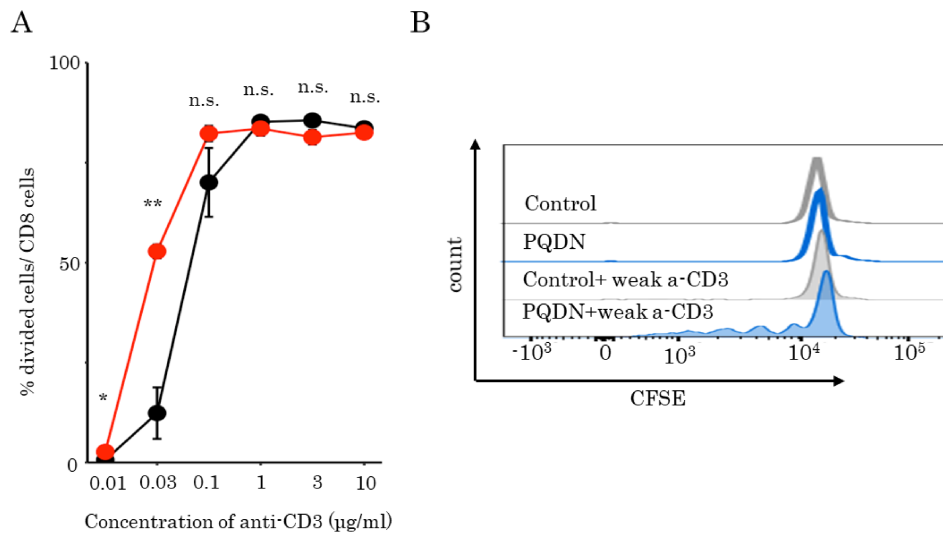
PCR and sequencing error correlations using the following parameter: ObadQualityThreshold = 10.

ROS detection using CellROX. Cells were seeded into 96-well plates at 1×10^5 cells/well. At each time point, cells were incubated with 250 nM CellROX (Thermo Fisher Scientific) for 45 min. The mean fluorescence intensity of CellROX was determined using flow cytometry.

Supplemental References:

1. Bolotin DA, Poslavsky S, Mitrophanov I *et al*: MiXCR: software for comprehensive adaptive immunity profiling. *Nat Methods* 2015, 12(5):380-381.

SUPPLEMENTARY FIGURES

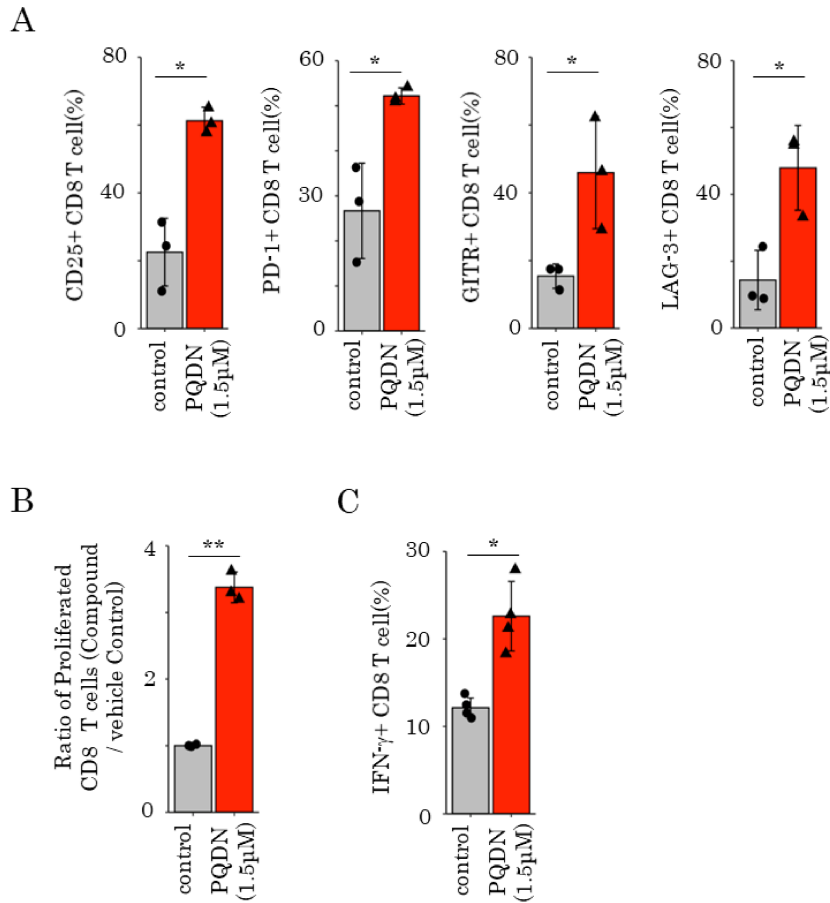
**Supplementary Fig. 1. PQDN enhances CD8 T cell activation even after weak TCR**

stimulation. A. Proliferation of CD8 T cells was evaluated when antigen stimulation was titrated

by using anti-CD3 antibody. **B.** Proliferation of DUC18 CD8 T cells after weak antigen

stimulation was measured using a CFSE dilution assay. CD8 T cells were stimulated with anti-

CD3 for 72 h in the presence of PQDN.



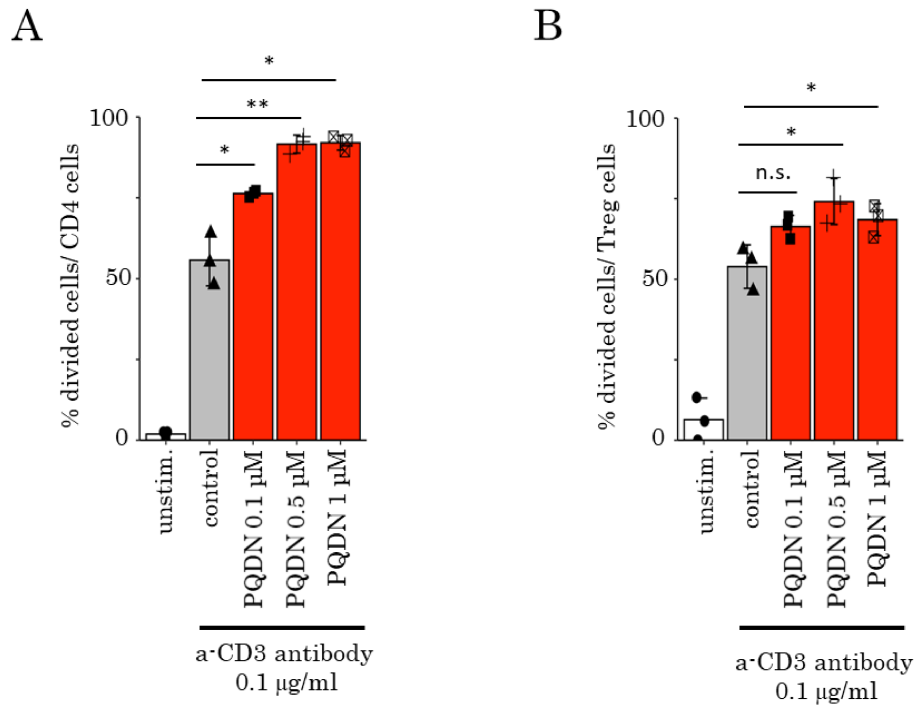
Supplementary Fig. 2. PQDN enhances CD8 T cell activation without antigen presenting

cells. A-C. CD25, PD-1, GITR, LAG-3 expression (A), proliferation (B) and IFN- γ secretion

(C) in CD8 T cells was measured by flow cytometry. Whole splenocytes from BALB/c mice

were stimulated using anti-CD3 for 72 h and treated with PQDN. Data represent means \pm SD

(n = 3-4 per group), unpaired Student's t-test.

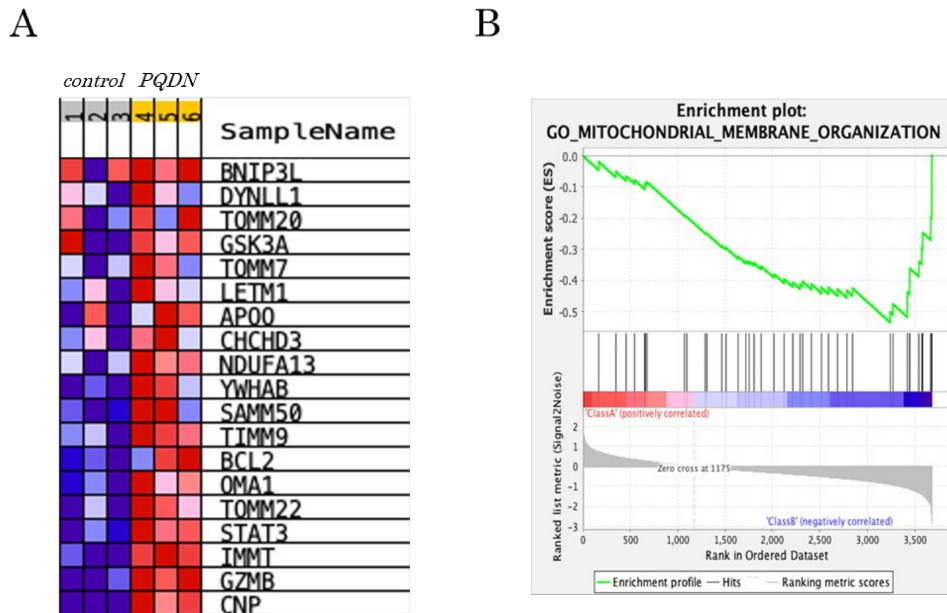


Supplementary Fig. 3. PQDN affects CD4 and regulatory T cells as well as CD8 T cells. A,

B. Proliferation of CD4 T cells (A) and regulatory T cells (B) from BALB/c mice stimulated with

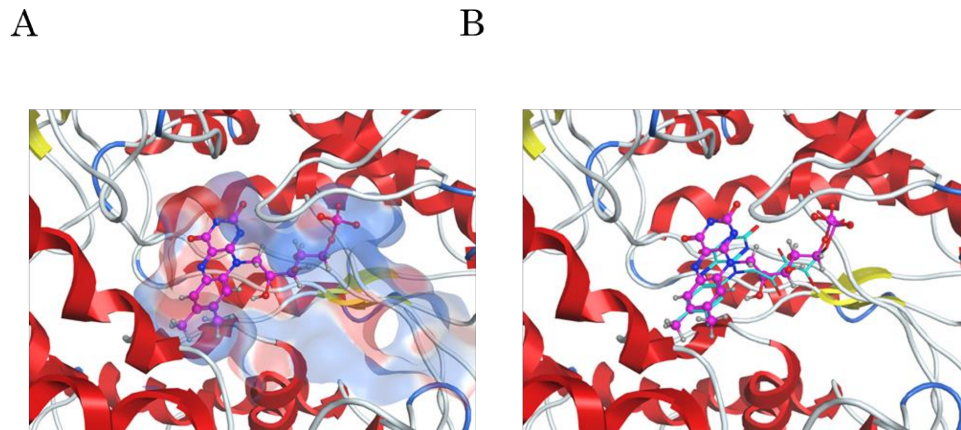
anti-CD3 for 72 h, and with PQDN were evaluated by flow cytometry. Data represent the means

± SD. (n = 3 per group), unpaired Student's t test.

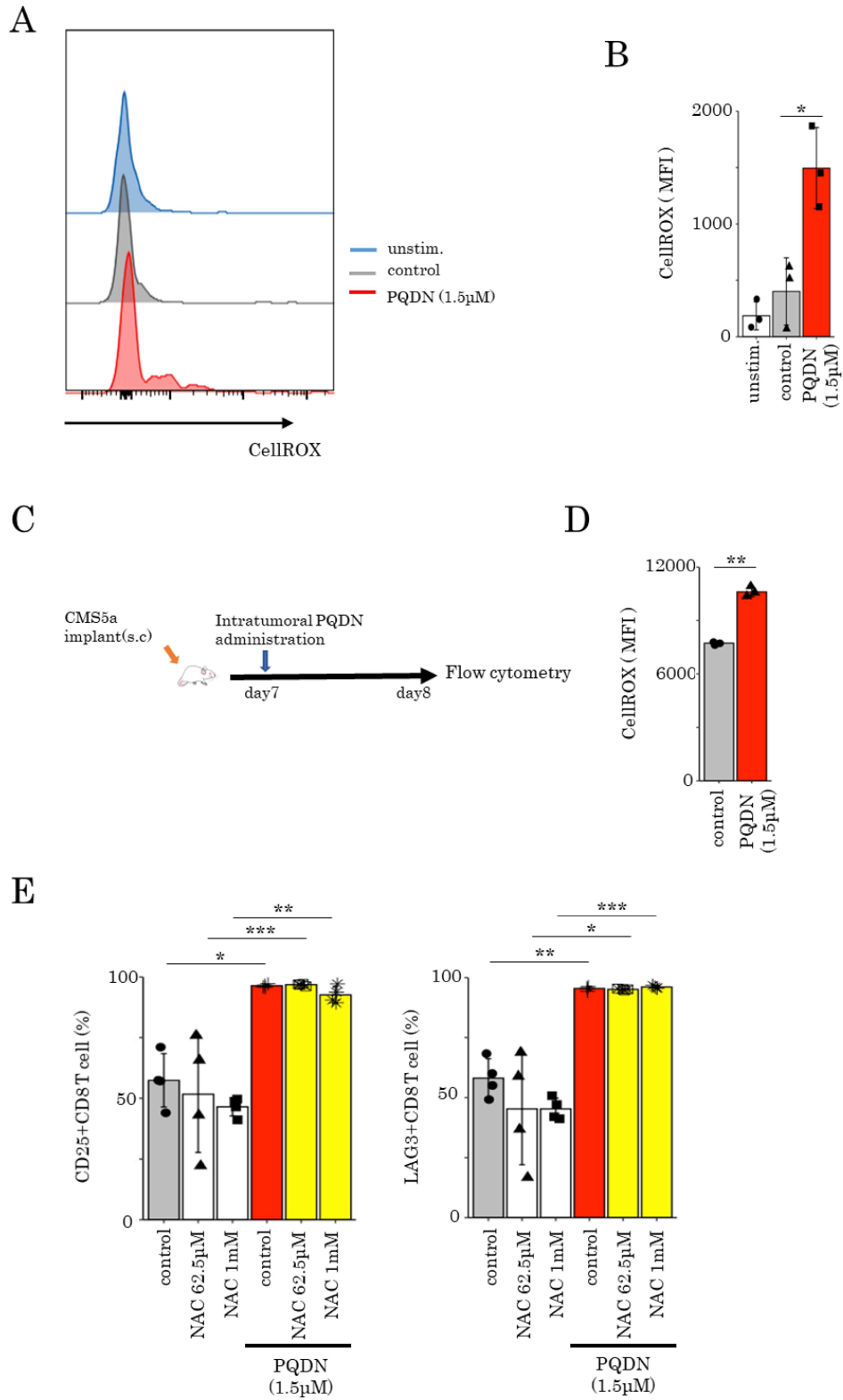


Supplementary Fig. 4. Cyclopedic gene expression in CD8 T cells treated with PQDN. A.

Whole splenocytes from DUC18 were stimulated with 9m peptide for 72 h and subjected to RNA-sequencing analysis. Heatmap representation of mitochondria-related gene expression (n = 3 per group). **B.** Subsequent Gene Ontology analysis showing mitochondrial membrane organization (n = 3 per group).

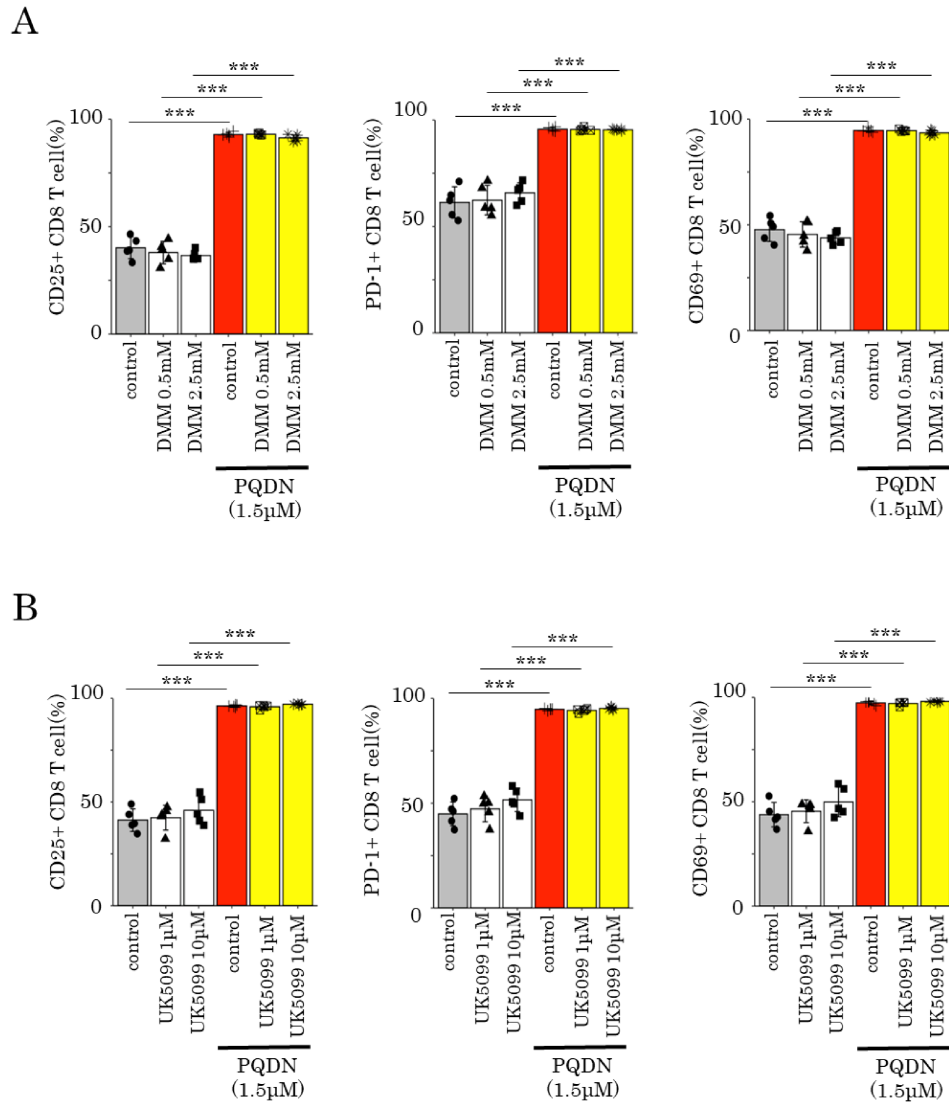


Supplementary Fig. 5. Docking model of FMN and redocked FMN. **A.** Docking model of FMN to a NADH dehydrogenase FMN-binding site of mouse mitochondrial complex I. The surface of the electrostatic map is shown using MOE. FMN is indicated in pink in ball-stick representation. **B.** Overlay of the original FMN and redocked FMN generated using MOE. Original FMN is indicated in cyan in line representation.



Supplementary Fig. 6. ROS is not involved in the effect of PQDN on CD8 T cell activation.

A and B. MFI of CellROX in DUC18 CD8 T cells stimulated with 9m peptide for 4 h. Data represent means \pm SD (n = 3 per group), one-way ANOVA with Tukey's post-test. **C and D.** CMS5a cells were subcutaneously inoculated into BALB/c mice. PQDN was intratumorally injected on day 7. MFI of CellROX in CD8 TILs at 24 h after administration. Data represent means \pm SD (n = 3 per group), unpaired Student's t test. **E.** Flow cytometric analysis of CD25 and LAG-3 expression in DUC18 CD8 T cells stimulated with 9m for 72 h using NAC. Data represent means \pm SD (n = 4 per group), unpaired Student's t-test.



Supplementary Fig. 7. PQDN augments CD8 T cell activation in a mitochondrial complex

II and mitochondrial pyruvate carrier independent manner. A. Flow cytometric analysis of

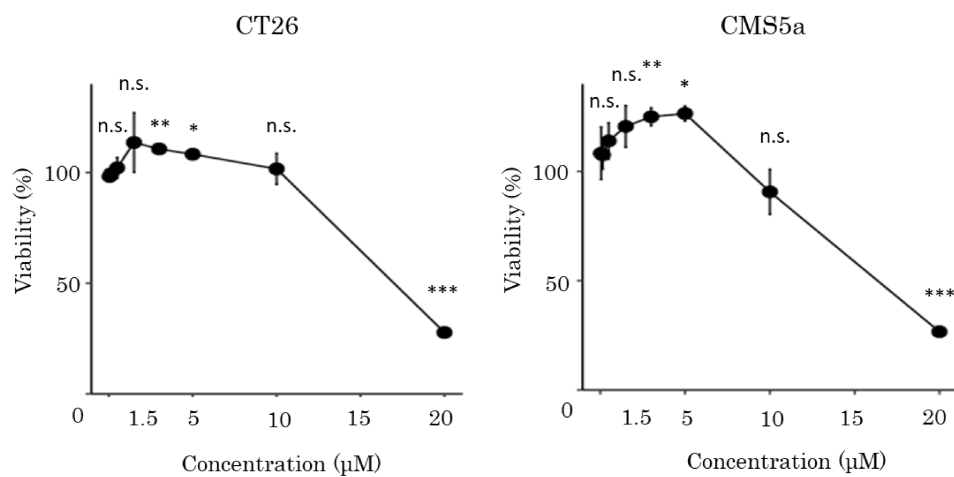
CD25, PD-1, and CD69 expression in DUC18 CD8 T cells stimulated with 9m for 72 h using

DMM. Data represent the means \pm SD (n = 5 per group), unpaired Student's t test. **B.**

Flowcytometric analysis of CD25, PD-1, and CD69 expression in DUC18 CD8 T cells

stimulated with 9m for 72 h using UK5099. Data represent means \pm SD (n = 5 per group),

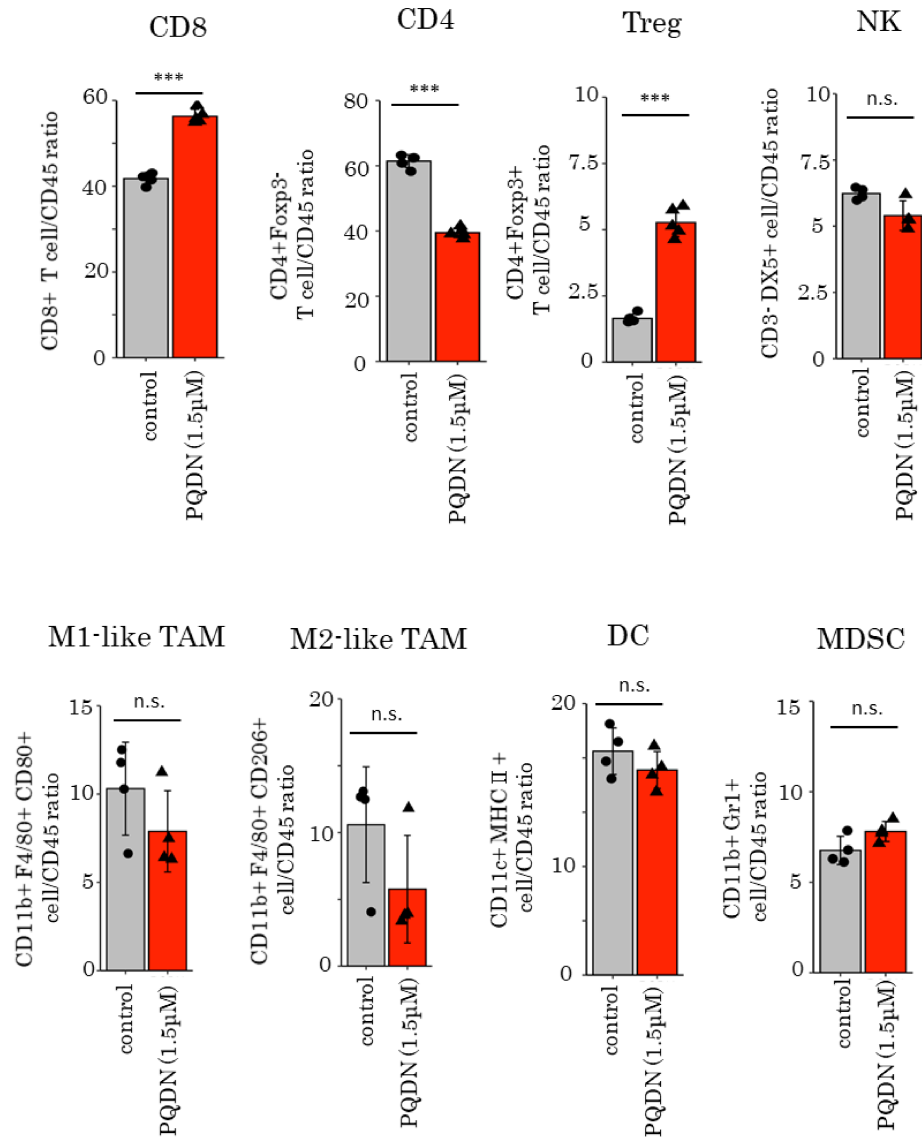
unpaired Student's t test.



Supplementary Fig. 8. CT26 and CMS5a cell lines show high resistance to the direct effect

of PQDN. A and B. Viability of CT26 and CMS5a cells treated with PQDN were evaluated for

WST8 assay. Data represent means \pm SD (n = 3 per group), unpaired Student's t test.

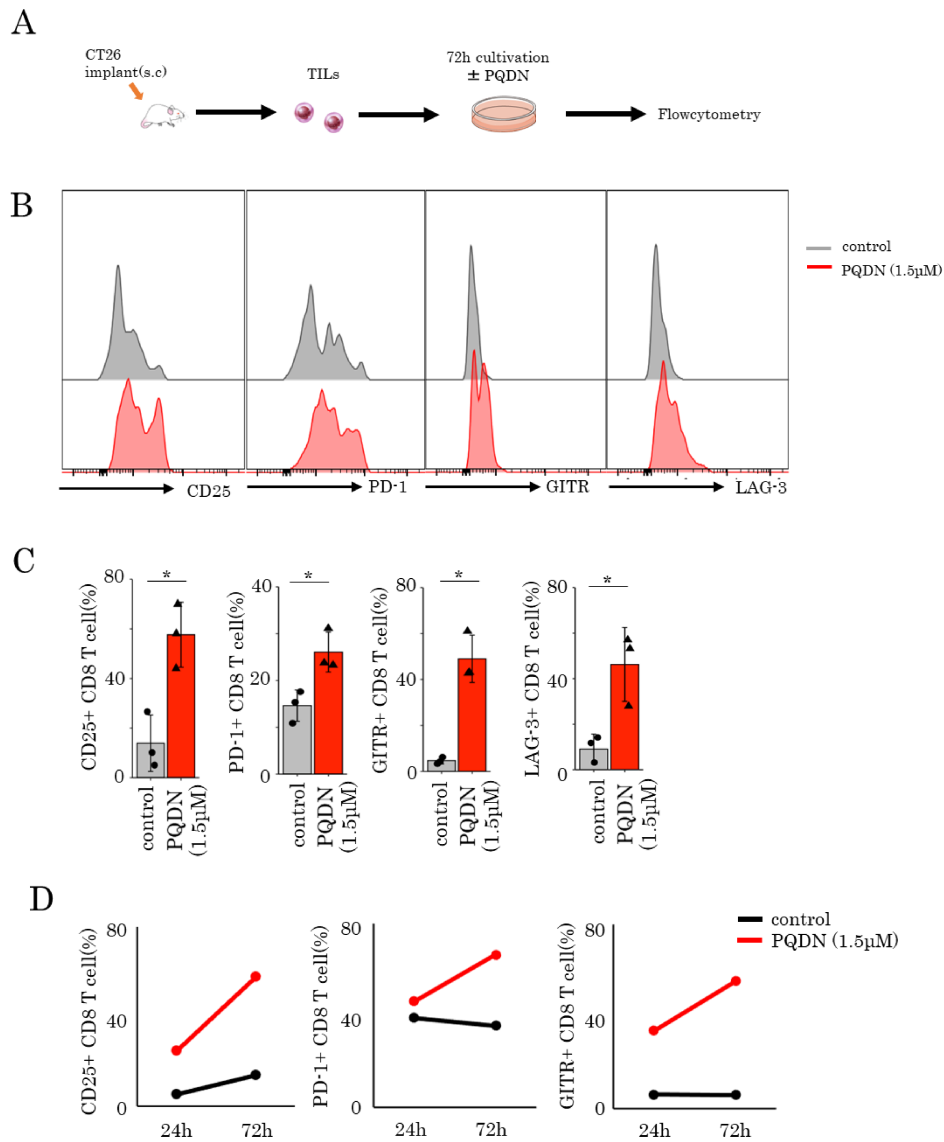


Supplementary Fig. 9. Population changes of immune cells treated with PQDN in the

CT26 tumor microenvironment. Each population changes of CD8, CD4, Treg T cell, NK,

TAM, DC, MDSC in the CT26 tumor when tumor-bearing mice were treated with PQDN were

evaluated. Data represent means \pm SD (n = 4 per group), unpaired Student's t test.



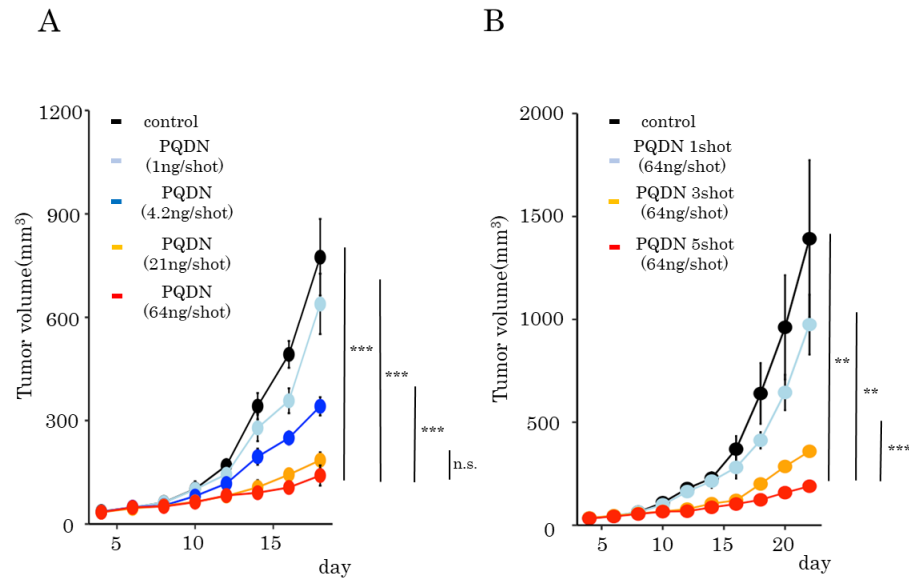
Supplementary Fig. 10. PQDN enhances the activation of CD8 TILs isolated from CT26

tumors. A–D. TILs from CT26 tumor-bearing mice were stimulated with anti-CD3 antibody

in the presence or absence of PQDN. **B and C.** Flow cytometric analysis of CD25, PD-1, GITR,

and LAG-3 expression in CD8 TILs were evaluated. Data represent means ± SD (n = 3 per

group), unpaired Student's t test. **D.** Flow cytometric analysis of CD25, PD-1, GITR, and LAG-3 expression in CD8 TILs from CT26 tumors, stimulated for 24 and 72 h.



Supplementary Fig. 11. Determination of optimal dose and times of PQDN in tumor-

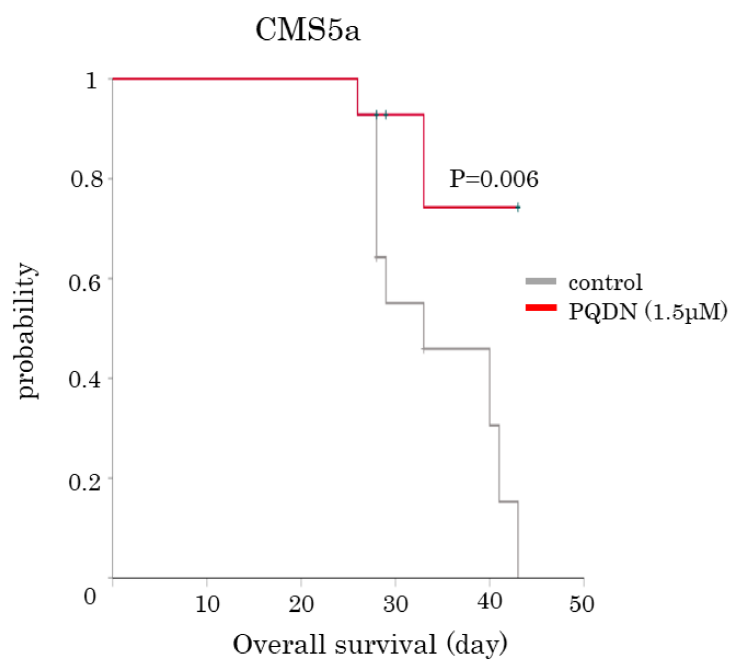
bearing mice. A. CT26-bearing mice were treated with intra-tumoral PQDN for each of PQDN

dose. Tumor sizes are shown ($n = 4$ per group) and analyzed using two-way ANOVA with Tukey's

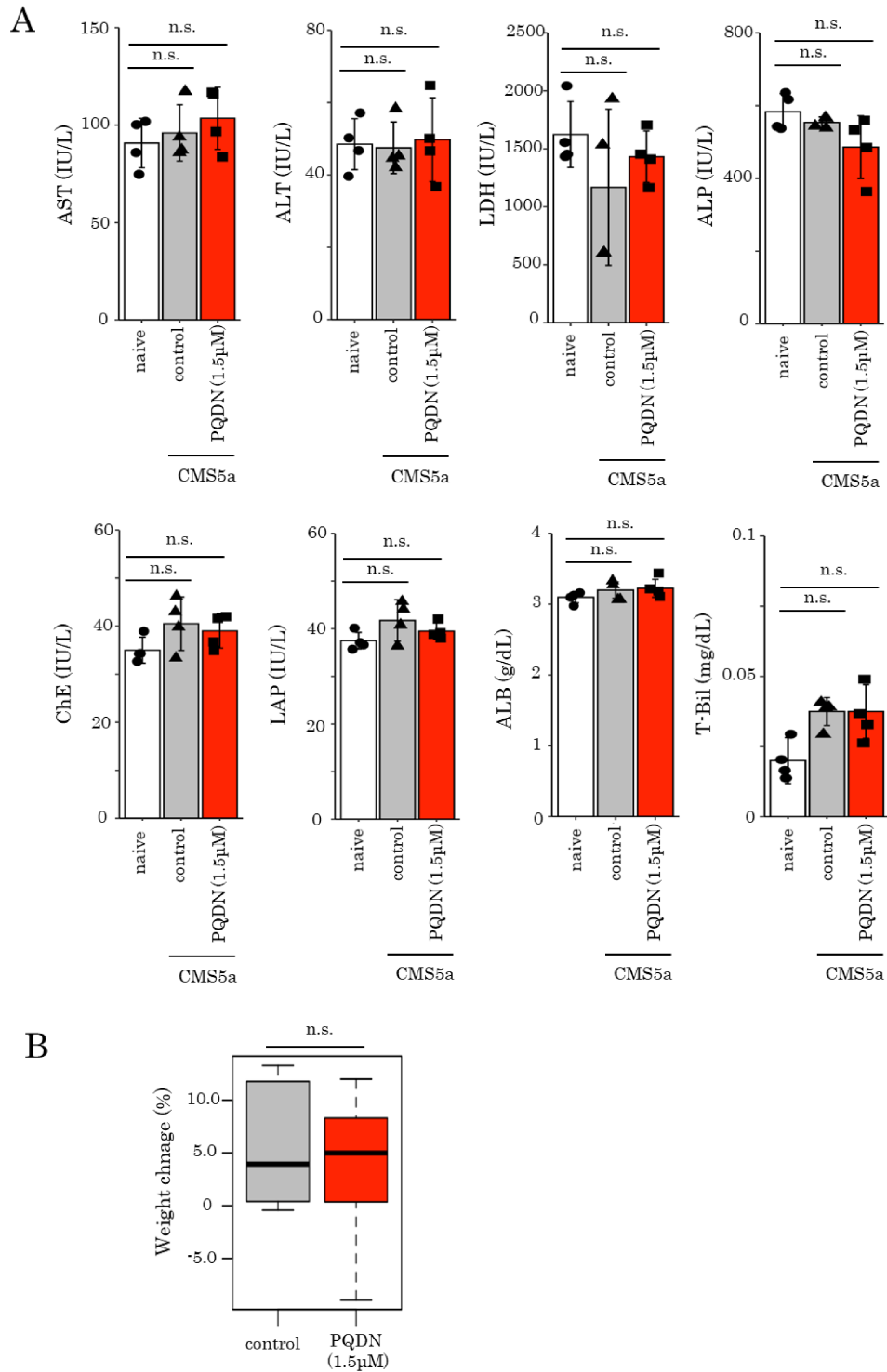
post-test. **B.** CT26-bearing mice were treated with intra-tumoral PQDN for each of PQDN time of

shot. Tumor sizes are shown ($n = 4$ per group) and analyzed using two-way ANOVA with Tukey's

post-test.

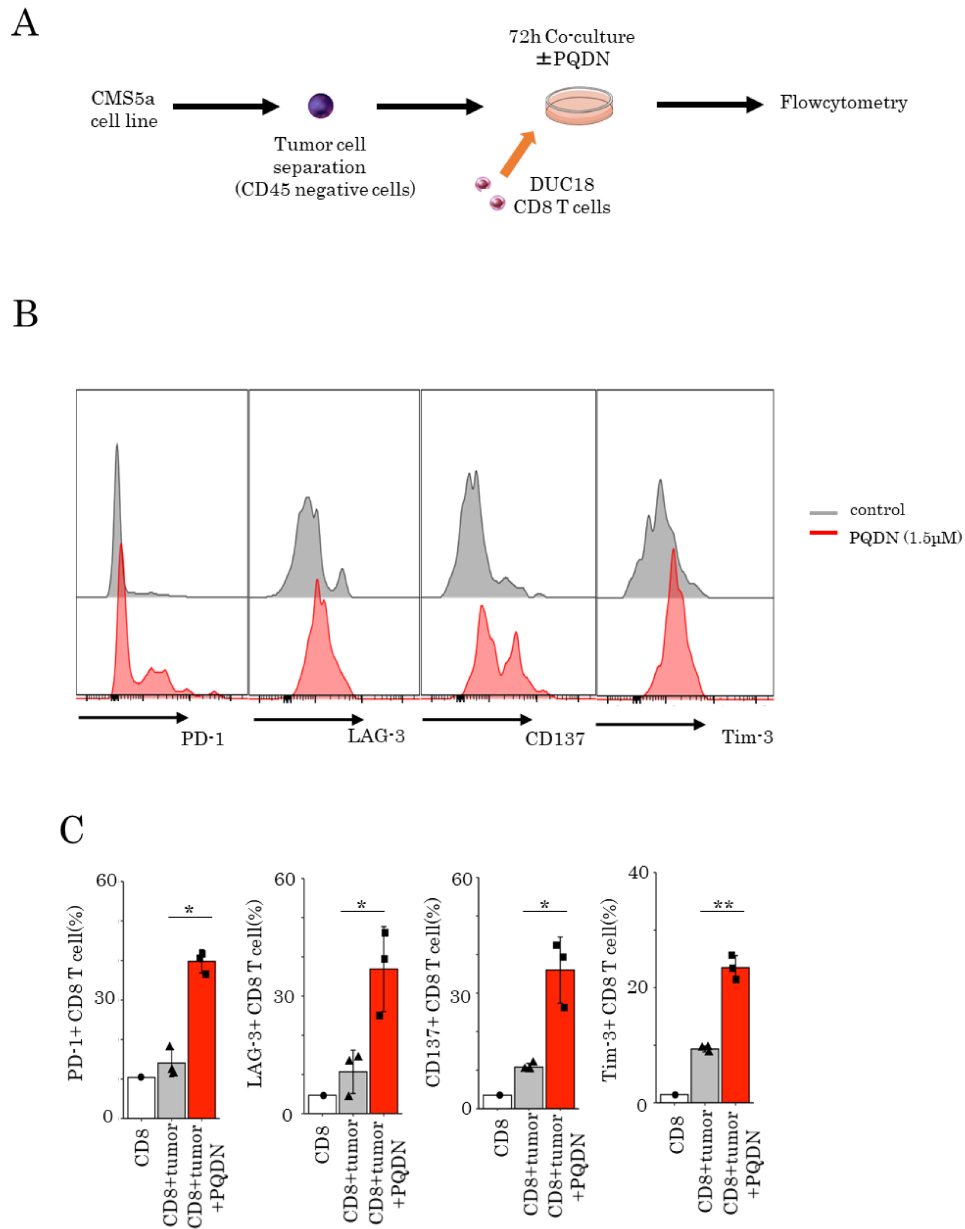


Supplementary Fig. 12. PQDN extends overall survival of CMS5a-bearing mice. Survival curves using the Kaplan-Meier method for CMS5a-bearing mice treated with PQDN. (n = 14 per group).



Supplementary Fig. 13. Intratumoral injection of PQDN does not exhibit the disorder of

liver function and weight loss of tumor-bearing mice. A. Examination of liver function in serum were performed in CMS5a-bearing mice treated with PQDN. Data represent means \pm SD (n = 4 per group), unpaired Student's t test. **B.** Weight change in CMS5a-bearing mice treated with PQDN on day18 compared with before treatment. Data represent means \pm SD (n = 8 per group), unpaired Student's t test.

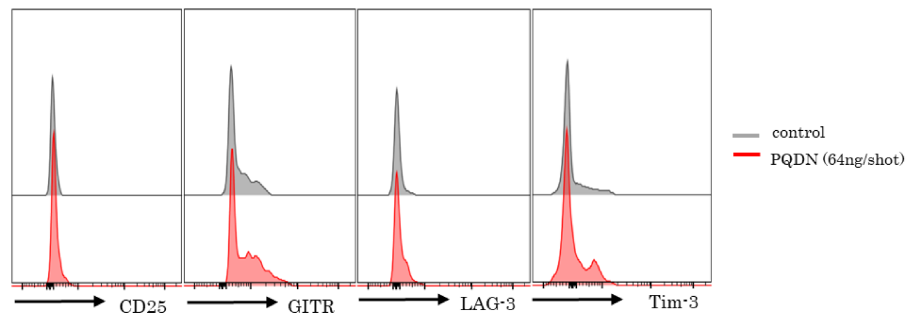


Supplementary Fig. 14. PQDN increases the direct recognition by specific CD8 T cells to tumor. **A-C.** CD8 T cells isolated from DUC18 mice were co-cultured with tumor cells from CMS5a tumor-bearing mice for 72 h. **B and C.** The expression of PD-1, LAG-3, CD137, and

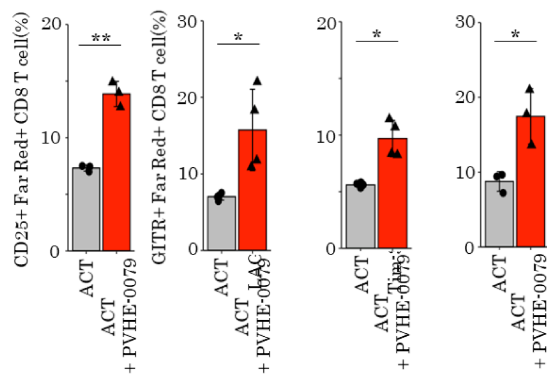
Tim-3 on cultured CD8 T cells was measured by flow cytometry. Data represent means \pm SD

(n = 3 per group), unpaired Student's t test.

A



B

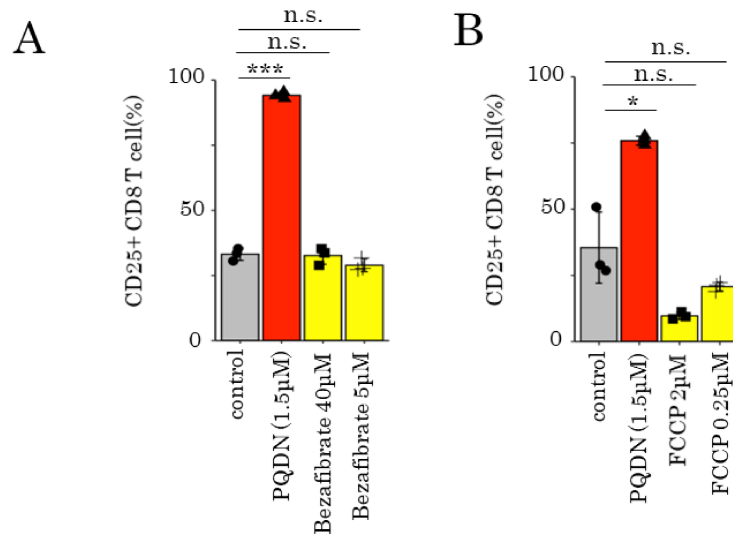


Supplementary Fig. 15. PQDN enhances the activation of tumor antigen specific transfused

CD8 T cells. A and B. Flowcytometric analysis of CD25, GITR, LAG-3, Tim-3 expression in

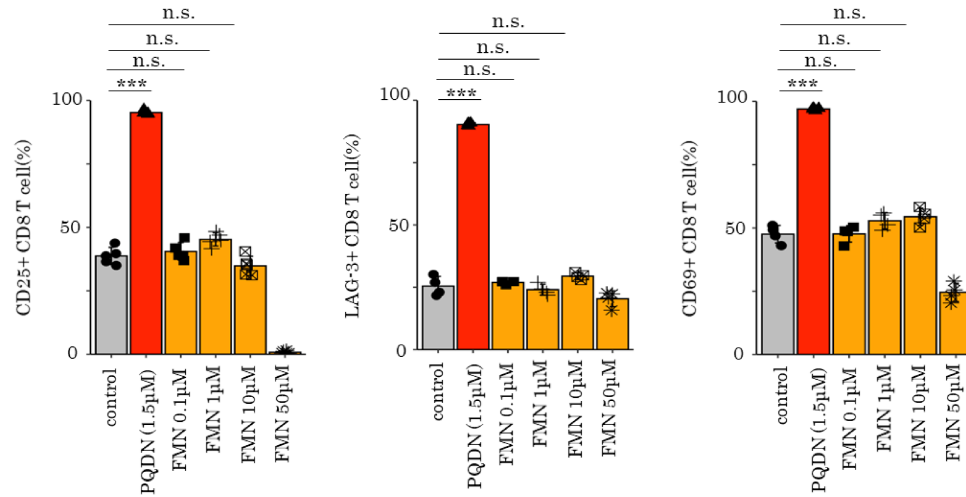
infused CD8 T cells at CMS5a tumor. Data are shown as mean \pm SD (n=3-4 per group) and analyzed

using unpaired Student's *t*-test.



Supplementary Fig. 16. Bezafibrate or FCCP does not enhance the activation of T cells

receiving weak stimulation. A. Flow cytometric analysis of CD25 expression in DUC18 CD8 T cells stimulated with 9 m for 72 h using bezafibrate. Data are shown as mean \pm SD (n = 3 per group) and analyzed using unpaired Student's *t*-test. **B.** Flowcytometric analysis of CD25 expression in DUC18 CD8 T cells stimulated with 9 m for 72 h using FCCP. Data are shown as mean \pm SD (n = 3 per group) and analyzed using unpaired Student's *t*-test.

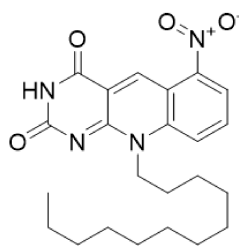


Supplementary Fig. 17. FMN cannot augment the activation of CD8 T cells after weak TCR

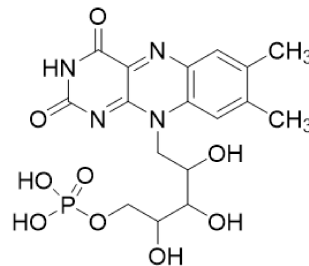
stimulation. Flow cytometric analysis of CD25, LAG-3, and CD69 expression in DUC18 CD8

T cells stimulated with 9m for 72 h using FMN. Data represent the means \pm SD (n = 4-5 per

group), unpaired Student's t test.



PQDN
CLogP: 6.31



FMN
CLogP: -2.61

Supplementary Fig. 18. ClogP value of PQDN and FMN. CLogP values were calculated by the

ChemBioDraw software 14.0.0.117.